THE ASTROPHYSICAL JOURNAL, 306:266–270, 1986 July 1

A COMPARISON OF HIGH-RESOLUTION RADIO AND OPTICAL DATA FOR THE NORTHEAST REGION OF THE CYGNUS LOOP

W. C. STRAKA
Lockheed Palo Alto Research Laboratory

J. R. DICKEL
Department of Astronomy, University of Illinois

W. P. BLAIR
Center for Astrophysical Sciences, The Johns Hopkins University

AND

R. A. FESEN
Laboratory for Atmospheric and Space Physics, University of Colorado
Received 1985 June 3; accepted 1985 December 23

ABSTRACT

Radio observations of the northeastern part of the Cygnus Loop obtained with the VLA at 18 cm with a resolution of 4.″7 are presented and discussed. The radio emission is compared to digitized optical images taken with Hα, [O III], [S II], and [O I] interference filters. In general, the brightest radio filaments match the brightest optical filaments very well, particularly those which are bright in Hα. The agreement in position, morphology, and relative brightness is particularly good where all four optical species are bright. However, a few bright radio features have no bright optical counterparts.

The general radio and optical structure of the region can be explained by a model in which shocked interstellar clouds form filaments due to unstable cooling and compression. The features appear to be ropelike, although it is not possible to rule out that they are irregular sheets seen edge-on. A large gradation in cooling on a scale of parsecs is evidenced by the sequence of the optical species in emission, with a corresponding increase in density generally evidenced by the continuum radio emission. After the filament cools, magnetic pressure and evaporation may become sufficiently high to disperse the filament.

In addition to filaments, there appears to be a diffuse component to the radio emission which may arise in the shocked intercloud medium.

Subject headings: nebulae: individual — nebulae: supernova remnants — radio sources: extended

I. INTRODUCTION

Observations have been available for some time showing a general correspondence between regions showing radio synchrotron emission and optical line emission in old supernova remnants (SNR). Van der Laan (1962) and Duin and van der Laan (1975) suggested that compression of filaments due to thermal instabilities would increase the magnetic field strength and relativistic particle density, thus enhancing the synchrotron emissivity. Relatively cool dense regions would also be the locations of the optical line emission. However, there have been few studies detailing the small-scale similarities in the radio and optical structure of these objects (Duin and van der Laan 1975; Dickel and Willis 1980). It is important to investigate if such presumed correlations between density and magnetic field strength persist in SNR at all scales down to the limit of discernable features.

Many galactic SNRs have optical filaments with widths of only a few arcseconds. Thus, radio observations with a resolution of this same order are required to test the exact structural correspondence between a remnant's optical and radio emission. We have carried out such observations on the northeastern section of the Cygnus Loop remnant (NGC 6992) using the Very Large Array of radio telescopes (VLA).[1] The resultant map of the radio emission is compared with interference-filter optical photographs taken in Hα, [S II], [O I], and [O III] (cf. Fesen, Blair, and Kirshner 1982, hereafter FBK). These data also provide information on the shape and structure of the emitting regions for comparison with theoretical models. The observations are presented in § II, and a comparison of the radio and optical data is given in § III. We discuss these results in § IV.

[1] The VLA of the National Radio Astronomy Observatory is operated by Associated Universities, Inc., under contract with the National Science Foundation.

II. OBSERVATIONS AND REDUCTIONS

a) Radio Data

The Cygnus Loop is so large (diameter ≈ 3°) that only a small fraction of it can be covered in a single observation with the VLA. At a wavelength of 17.8 cm, the half-power beamwidth of the individual antennas is slightly less than 30′. Even this field cannot be fully mapped because of bandwidth restrictions. As a compromise between the needs for both large (to achieve a good signal-to-noise ratio) and small (to achieve a large field of view) bandwidths, we observed in six frequency channels, each 6.25 MHz wide, centered about 1652 MHz. This provides a response which remains greater than 95% of the peak value out to an angular radius of 5.′3. Limitations to the storage of data in the computer required that each of the six channels be processed independently, then added together to produce the final map displayed in Figure 1 (Plate 15) and superposed on a [S II] photograph in Figure 2 (Plate 16). The

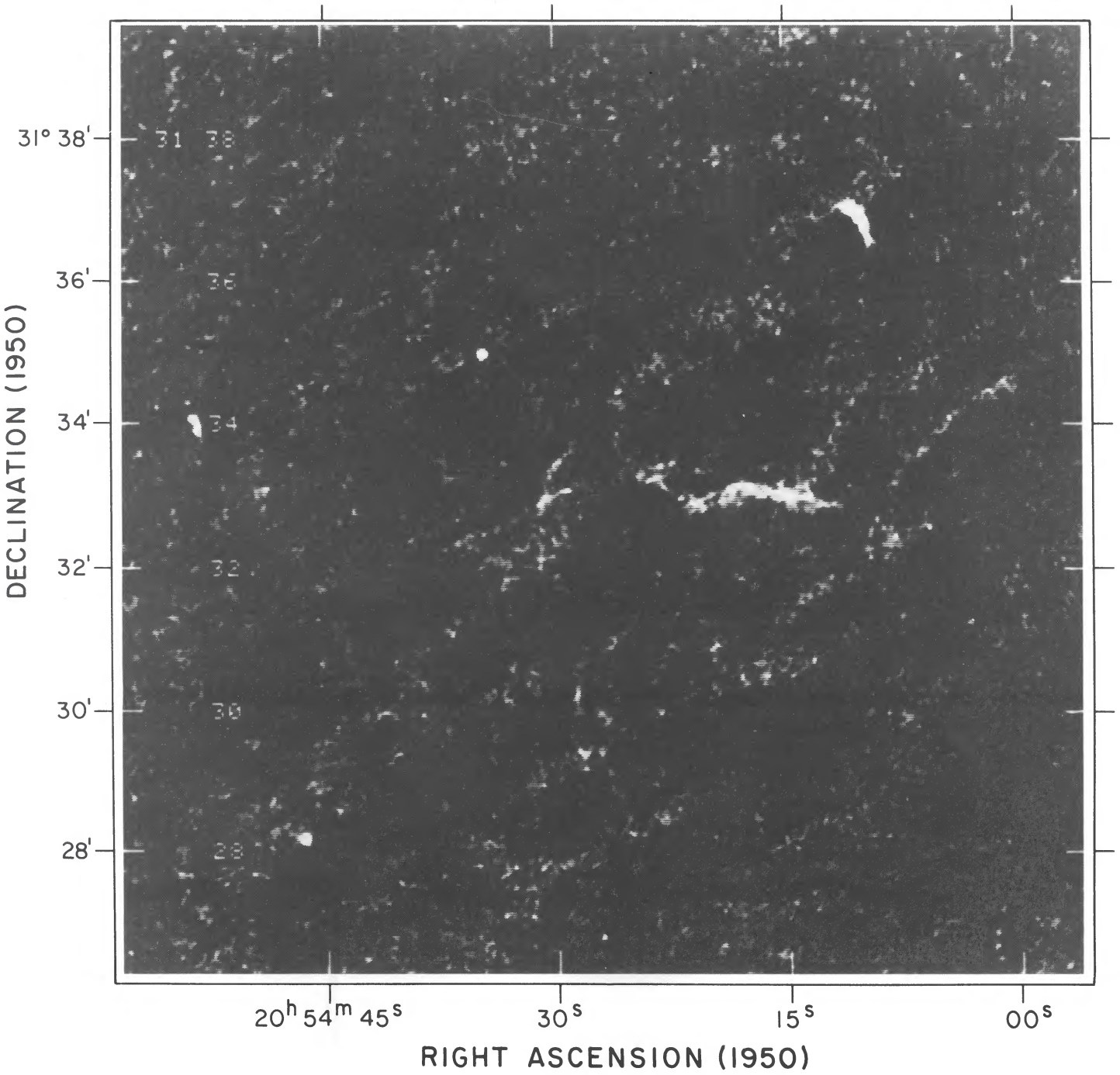

FIG. 1.—Radio image of the northeastern region of the Cygnus Loop supernova remnant (NGC 6990). This image was obtained with the VLA in the B configuration at 17.8 cm, with subsequent image processing. The half-power beamwidth is 4.″7.

PLATE 16

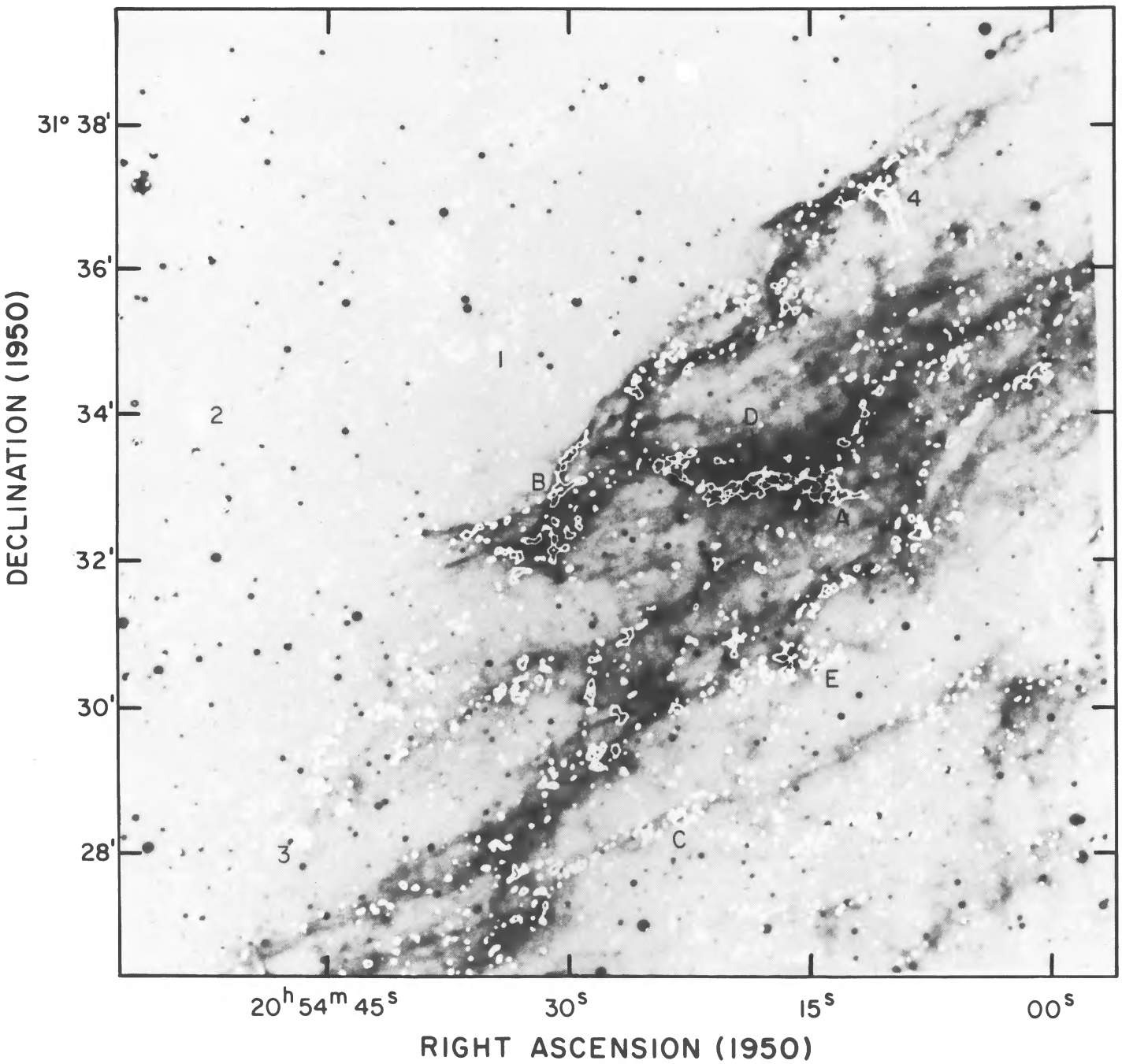

FIG. 2.—Contour map of the radio emission from the northeast corner of the Cygnus Loop measured at a wavelength of 17.8 cm using the VLA, superposed on the [S II] image of the region obtained by Fesen, Blair, and Kirshner (1982). The contour interval of the radio map is 0.12 mJy beam^{-1}, and the half-power beamwidth is 4".7. Note the excellent agreement of the brighter radio features with the brighter [S II] features, particularly near the center of the image. The numbers indicate radio sources listed in Table 1, while the letters indicate features discussed in the text.

original maps covered an area 4096″ on a side, centered at a position of R.A. $20^h54^m50^s$ and decl +31°33′00″ (1950). For display purposes, we show an area 800″ on a side centered on the brightest region of the shell in this northeastern edge of the SNR.

The data were obtained with the standard B configuration of the VLA, giving a synthesized half-power beamwidth of 3.″3 at this wavelength. After CLEANing, the maps were restored with a circular Gaussian beam having a half-power beamwidth of 4.″7. In this fairly extended configuration of the VLA, there are few short spacings between antennas. Thus, the response of the system is incomplete, and structures larger than about 1′ are missing from the map.

The residual stripes visible on the final map are caused primarily by the strong source CL 7 (Keen *et al.* 1973) at a position of $20^h55^m56^s.4$ and 31°30′51.″1, with a flux density of about 600 mJy. This source lies outside the region of the map shown but was in the original map near the half-power point of the primary beams of the individual antennas. Because CL 7 lies on the steepest gradient of the primary beam patterns and is somewhat distorted, the standard CLEAN and self-calibration routines were unable to remove its effect completely.

In order to determine the reality of features in the radio map, tapered box and median filter algorithms were applied to the data. The results indicated filamentary structure down to the original resolution limit (3.″3), with hints of more detail at the noise level. We estimate that all features brighter than 0.25 mJy per beam (about 3 times the rms noise level on the map) are real. This includes features A, B, E, parts of the curved arcs to the northwest and southwest of A, the emission about 2′ northeast of C and 15^s east of E, and the emission from the filament between A and B. While there are probably real but fainter features present, we did not attempt to pick them out from the noisy background.

We also note that the bright extended source (labeled 4 in Fig. 2) at $20^h54^m10^s.3$ and 31°36′55″ in the northern part of the map resembles a head-tail source and is very likely a background object. We can, therefore, say nothing about the emission from the SNR at that position. This and three other point sources in the field are listed in Table 1 and identified on Figure 2. No identification of these sources has been made.

b) *Optical Data*

The radio data were compared to optical images which were taken as part of a series of narrow-band filter photographs obtained with the 144 mm single stage ITT image tube on the f/7.5 focus of the 1.3 m telescope of the McGraw Hill Observatory (cf. FBK). Narrow passband interference filters were employed to isolate the emission lines of Hα + [N II], [O III], [S II], and [O I] (see Table 2).

The plates were digitized on a 20 μm grid (0.″2) then compressed to a scale of 2″ per pixel to match the VLA data and the 512 pixel square display used with the DIDCS2 image processing system at NASA/Goddard Space Flight Center. Astrometry was done by interpolation of the positions of two stars in the field which appear in the SAO catalog (SAO 070707 and 070698). Using the solution from these positions, we accurately reproduced the coordinates of Miller's (1974) slit position 1. There remain some slight geometric distortions due to minor differences in the plates and a change in the ITT image tube between observing runs. Mismatches in position were not apparent in the star images when the Hα, [S II], and [O I] images were overlaid, while a slight mismatch (less than a star image diameter) remains when overlying the Hα and [O III] images. Positioning is therefore accurate to a fraction of a pixel, but separations between optical features were considered significant only when greater than a pixel width (2″), or the final beamwidth (4.″7) when comparing with radio images.

No calibration spots or standards were available. Further, there are density variations across the plates due to discoloration from residual fixer. We also note that the Hα image contains the emission of the adjacent [N II] lines. Variations in the [N II]/Hα ratio could affect the intensities measured on the Hα plate. FBK found relatively small variations in this ratio (±20%), and the spatial extent of Hα and [N II] in well-evolved SNR is usually quite similar. We will refer to this image as the Hα image for brevity, but the reader should keep the [N II] emission in mind.

TABLE 1

SMALL DIAMETER RADIO SOURCE IN THE NORTHEAST FIELD OF THE CYGNUS LOOP

Source Number	R.A.(1950)	Decl.(1950)	Comments
1	$20^h54^m35^s.1$	+31°35′05″	...
2	20 54 53.7	31 34 02	double
3	20 54 46.5	31 28 11	in optical filament
4	20 54 10.3	31 36 55	head-tail, in optical filament

TABLE 2

SUMMARY OF THE OPTICAL IMAGERY[a]

Optical Line	Central Wavelength of Filter (Å)	Bandwith (FWHM) (Å)
Hα + [N II]	6570	75
[O III]	5010	28
[O I]	6300	30
[S II]	6736	50

[a] See FBK for a complete discussion of these images.

III. RADIO AND OPTICAL RESULTS

a) *Radio*

From inspection of the radio map, we see that the emission appears to be concentrated largely into thin filaments analogous to those seen in the optical. Most of the radio structures are found to be somewhat thicker than the instrumental resolution, with deconvolved widths ranging from about 3″ to 12″. A typical value is about 6″, corresponding to a linear diameter of about 0.02 pc at an adopted distance to the Cygnus Loop of 770 pc (Minkowski 1958). There is no correlation between the thickness of a given feature and its apparent brightness.

The lengths of the filaments are often tens of times their widths. While many of the filaments appear to be oriented tangentially to the overall shell, a few notable ones have very different alignments, such as the bright, somewhat S-shaped structure near the center of the map (feature A; see Figs. 1 and 2), which appears to be several filaments seen together. Straka (1986) has noted on the basis of numerical models of cloud-shock interactions that supernova shocks will be bent in the vicinity of clouds to give a range of angles with respect to the line of sight. This will create a wrinkled structure of density

enhancements which can appear as filaments with various orientations.

To determine whether all the emission is tied up in small-scale structures or whether there may be an underlying smooth component ($>1'$), like that indicated in a lower resolution map of the southwestern region of the Cygnus Loop (Green 1984) and which would have gone undetected with the configuration of the VLA used, we have compared the present map of NGC 6990 with one made at a resolution of $56'' \times 107''$ by Dickel and Willis (1980) at a wavelength of 49 cm using the Westerbork Synthesis Radio Telescope. To calculate the expected flux density at 17.8 cm, we scaled the Westerbork map by a factor of 0.60, which is the ratio of the total flux densities at these wavelengths in the spectrum published by DeNoyer (1974). (A change in the spectral index of 0.2 will change the ratio by about 20% of its value.) Measured values were determined at several locations on the present map by integration of the brightness over the area of a Westerbork beam, centered at the given position. The true zero level for this integration is uncertain because of the missing spacings in the VLA data. An adopted base level was chosen as the mean brightness at positions where there were no obvious radio filaments, typically -0.03 mJy (VLA beam)$^{-1}$. If there were no filaments present within a Westerbork beam, this value for the baseline would be uncertain by:

$$\frac{\text{rms noise}}{\sqrt{\text{VLA beams per Westerbork beam}}} \text{ or } \frac{0.08}{\sqrt{271}}$$

$$= 0.005 \text{ mJy beam}^{-1},$$

but because of the irregular structure of the SNR, we adopt a value of twice this amount or a 3 σ uncertainty of 0.03 mJy (VLA beam)$^{-1}$.

In the regions where we see filaments on the shell, our measured flux densities were about half the values expected from the Westerbork map. If much of the emission were in very faint filaments similar in thickness to the detected ones, but with a surface brightness below the noise level, their brightness should still be included in the integrated flux density. If the maximum uncertainty discussed above for the baseline and the steepest choice of spectral index are adopted, the integrated VLA flux density could reach three-fourths of the Westerbork value for the brightest point on the SNR and about 85% at the other selected spots. Therefore, we conclude that roughly one-half of the radio emission from the Cygnus Loop may be in a smoothly distributed structure with a scale size greater than $1'$–$2'$. Without calibrated low- and high-resolution data at optical wavelengths, we cannot tell if there is also such a diffuse component to the optical line emission.

Can the two distinct components—apparent filaments and smooth—represent sheetlike structures seen edge-on and face-on, respectively? The analysis of Smith and Dickel (1983) showed that the break-up of sections of an initially thin shell by thermal instabilities can result in structures which are still thin in relation to their extent. Green (1984) and Dickel and Willis (1980) have used the presence of a particularly long filament seen across nearly the center of the Cygnus Loop and a similar one in the remnant CTB1 to argue against such a possibility. The observed shapes of such sections will depend critically on the viewing angle and should show a decrease in surface brightness with increasing width which is not observed. Although there may be irregularities in emissivity and depth of sheets which could mask such a correlation, there is certainly no evidence for sheet-like structures in the radio emission from the Cygnus Loop. From analysis of the optical emission, Miller (1974) concluded that the depths of the observed features were between 1 and 10 times their observed widths.

The small-scale features producing the filamentary emission may be a combination of shocked clouds (Blandford and Cowie 1982) and zones which have been further compressed by thermal instabilities within the shell (Cox 1972; Duin and van der Laan 1975). To evaluate their parameters we shall assume that they have depths which are 3 times their observed diameters. The surface brightness of the brighter filaments is typically 0.3 mJy beam^{-1}. If the radiation is isotropic, then the luminosity $L(18 \text{ cm}) = 2.01 \times 10^{17}$ ergs s^{-1} Hz^{-1} within a column outlined by the 4.″7 diameter beam. If we choose a line-of-sight thickness equivalent to 10″, or 1.12×10^{17} cm, the density of luminous energy per unit frequency is 6.5×10^{-34} ergs cm^{-3} s^{-1} Hz^{-1}. Integrating over frequency from 1 MHz to 100 GHz with a spectral index of -0.5, we find the luminous energy density to be approximately 10^{-26} ergs cm^{-3} s^{-1}. If the relativistic particles produce synchrotron radiation at this rate for an estimated lifetime of 85,000 yr (from the formulae compiled by Lang 1978), then the total relativistic energy density is about 3×10^{-14} ergs cm^{-3}, or the pressure in relativistic particles is 10^{-14} dynes cm^{-2}, much less than the magnetic and gas pressures ($\sim 10^{-9}$ dynes cm^{-2}).

b) Optical

In general, the brightest filaments seen in the optical images through each interference filter are also visible in the others. As discussed by FBK, the [S II] image is virtually a copy of the Hα one (although some small variations in relative intensity are present) and the [O I] emission is quite weak. Thus, most of our discussion will be concerned with the Hα and [O III] images.

There is a strong positional gradient of excitation across the shell of the Cygnus Loop (cf. FBK). This is readily apparent in a comparison of [O III] to Hα (Fig. 3 [Pl. 17]). The [O III] emission is generally found farther out from the center of the remnant than is the emission in the other lines. Regions showing stronger [O I] emission are found farther inward than those which are bright in Hα and [S II]. As the remnant expands, we find the most recently shocked material on the outside, whereas farther in, the material has had time to cool and compress into denser filaments.

In addition, there appears to be a displacement of excitation within individual filaments such that the maximum of the [O III] emission is displaced toward the leading edge of the filament relative to the Hα and [S II] maximum. The magnitude of this displacement of the [O III] maximum for a given filament is often of the same order as the resolution in the digitized images, but is systematically in the direction of apparent shock motion for filaments of differing orientations. This systematic dependence of direction on orientation of the filament suggests that there may be a real effect of nonaxisymetric excitation within an individual filament. The current analysis shows that Hα and [S II] structures range from the limit of resolution up to 6″ in angular width across an individual filament and often appear to have a slightly greater angular width than the [O III] filaments. Unfortunately, plate irregularities preclude a better evaluation of this phenomenon at present.

c) Comparison of Optical and Radio Emission

There is a strikingly good overall correlation of the optical structure and those individual radio filaments significantly

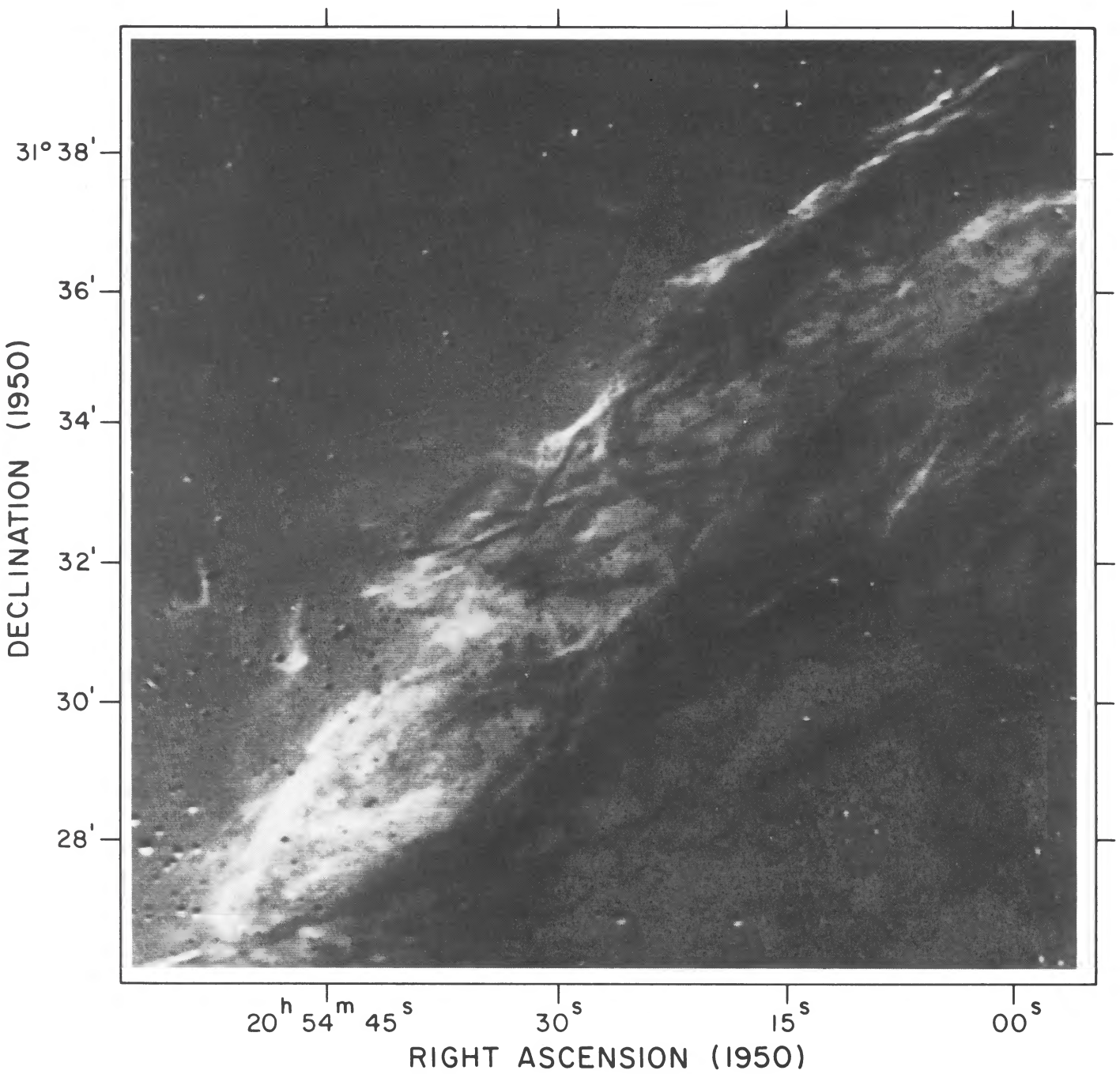

FIG. 3.—[O III] – Hα. This image was obtained by subtracting the Hα image of the northeastern rim of the Cygnus Loop from the [O III] image, using the DIDCS2 image processing system at NASA/Goddard SFC. [O III] is shown as light with Hα shown as dark. Note that the major regions of [O III] lie outside the Hα structures. This image represents the difference in plate density only and not the actual brightness of any filament. Note also that there is often a shift in the position of the [O III] peak relative to the Hα peak for a given filament.

STRAKA, DICKEL, BLAIR, AND FESEN (*see* page 268)

brighter than the background noise (Fig. 2). This result extends the agreement found by early work on the Cygnus Loop (Moffet 1971; Keen *et al.* 1973; Dickel and Willis 1980) to an order of magnitude better resolution. The best match of optical to radio is in regions where all four optical emission lines are bright. Otherwise, Hα generally provides the best correlation with the radio structure. This suggests that the filaments are presently of moderate electron temperature and were probably the areas of greatest initial density or are currently compressed the most.

The optical-radio correlation appears to extend to many of the faint features as well. Although the reality of any individual region of radio emission near the noise level cannot be firmly established, there is an overall impression that many of the radio spots connect into structures which match the Hα filaments. A good example is the long thin filament designated C near the southern side of Figure 2. Other features would include those which appear to be continuations of filamentary structures which are well above the background level. This agreement supports the interpretation that as these filaments have cooled and condensed the relativistic particle content and frozen-in magnetic fields have also been compressed to enhance the synchrotron emissivity.

The volume emissivity of radio synchrotron emission is proportional to $K \cdot B^{1-\alpha}$, where K is the density of relativistic particles, B is the magnetic field strength, and α is the spectral index for a power-law spectrum in which the flux density is proportional to frequency$^{\alpha}$. Detailed polarimetry to ascertain the orientation of the magnetic field is unavailable, and without it we cannot tell how the material contracts relative to the field. We have therefore assumed that the relativistic particles and magnetic field are both linearly dependent upon the density of thermal particles. The emissivity is then proportional to the $2 - \alpha$ power of the density. The radio spectrum of the Cygnus Loop is not well established, particularly at high frequencies, but for the frequencies of interest here a reasonable value of α is -0.5 (DeNoyer 1975). Thus the radio emissivity should be approximately proportional to density$^{2.5}$. The Hα emission should depend upon density squared. Thus even with uncertainty for the temperature and the magnetic field variations with density the emission in the two wavelength bands should track reasonably well.

A number of the radio features are resolved and appear to be somewhat wider than their optical counterparts. As filaments contract, the magnetic pressure will increase until it equals the gas pressure thus halting the compression. For a magnetic field strength of 30 μG and a density of 100 atoms cm^{-3}, the balance will occur at a temperature of 10^4 K. After the compression stops, a feature will be cool in the center but may get heated from the outside by the surrounding diffuse material in the hot shell. Such a temperature gradient could make the part which is visible in Hα appear thinner than that seen in the radio and also account for the relative differences seen in [O III] and Hα across individual filaments (see Straka 1986).

As previously seen in lower resolution maps (Dickel and Willis 1980; Hester, Parker, and Dufour 1983), there are some notable exceptions to the apparent correspondence between radio and optical emission. The bright optical filament, D, just to the north of the thick S-shaped feature (A in Fig. 2) is prominent in both Hα and [O III], but is just at the noise level if present at all in the radio data. On the other hand, there is a diffuse patch of radio emission (E) on the inner side of the shell at a position of $20^h54^m18^s$ and 31°30′30″ which has no bright optical counterpart. It would appear, therefore, that the density of the shocked material (≈ optical emission) and magnetic field strength (≈ radio emission) do not always follow one another on both small and large scales. Supporting evidence for this statement comes from the comparison of the densities measured toward two filaments: feature A and the filament just to the north of source 4 (see Fig. 2). FBK find a density in filament A which is less than one-third that in the filament north of source 4 as found by using the ratios of the same lines from Parker's (1964) data, yet the radio surface brightness toward A is about twice as bright as toward the northern filament. Spectrophotometry yielding the densities of more filaments is needed before a definitive conclusion about the relation of the radio emissivity to the density can be reached. Possible causes of the apparent discrepancies can be variations in the magnetic field strength of different regions of the preshocked gas, the squeezing of relativistic electrons out of dense regions during their compression, and compression with various orientations relative to the magnetic field so that the field strength and density do not follow directly. Although we cannot demonstrate the latter point with high resolution, low resolution polarimetry of old SNR shows a very random orientation of magnetic fields relative to the expansion of a remnant (e.g., Dickel and Milne 1976). Furthermore, in regions of moderate density, shock acceleration of relativistic particles might increase the synchrotron emission above that expected from compression alone.

The compression of the magnetic field and density in the postshock material can explain the generally good radio/Hα agreement seen in this small area of the Cygnus Loop, but it cannot account for the strong radio emission from the bright [O III] filament across the face of the remnant mentioned above or the entire western edge of CTB1 where the optical emission is all [O III] and the radio emission is brightest (Dickel and Willis 1980; Landecker, Roger, and Dewdney 1982). Perhaps these features are preexisting filaments in the interstellar medium with strong magnetic fields but relatively low densities which have just been shocked by the supernova.

IV. CONCLUDING REMARKS

The radio observations presented here represent a significant increase in the angular resolution with which radio features have been seen in SNR. They allow for the first time a detailed comparison of individual filaments at radio and optical wavelengths. Excellent agreement is usually found for filaments seen in both wavelength bands although differences in relative intensity do exist. Cooling and contraction of instabilities in the shocked clouds to increase the optical line emission also compress the frozen-in magnetic field to likewise increase the synchrotron emissivity at radio wavelengths. Observed differences in relative optical and radio intensities are probably the result of variations in the initial magnetic field strength of the preshocked clouds. In addition to the filament-like structure, there appears to be a smooth component to the radio emission which may arise in the diffuse intercloud medium which has been compressed by the expanding shock.

Finally, there is a decrease in radio emission interior to the region of bright Hα filaments but where optical [O I] emission is prominent. The expected lifetimes of the relativistic electrons (~85,000 yr) is significantly greater than the time to cool from having been shocked to producing predominantly [O I] emission (2000–4000 yr; Straka 1986) so we cannot be observing just the decay of the synchrotron radiation. Perhaps the

density in the inner region was more diffuse prior to the passage of the supernova shock so that the radio emissivity (Blandford and Cowie 1982) was always lower. Alternatively, there may be some mechanism to reduce the density and magnetic field strength in the regions of these [O I] filaments (see Straka 1986). Within the interior bubble of the remnant, evaporation and heating of filaments by conduction will occur rapidly. The coolest and densest filaments and similar parts of a given filament will disappear last. Thus the fragmentary and diffuse filaments visible in [O I] are the last vestiges of the compressed cloudy shell, most of which has already been dissipated.

We acknowledge the valuable aid of T. R. Gull and D. A. Klinglesmith of NASA/Goddard Space Flight Center in the use of the DIDCS2 Image Processing System, as well as helpful discussions. Some illuminating comments were also provided by J. J. Hester. We thank the referee for valuable suggestions and for asking us to firm up the presentation in several places. Support was provided in part by the NASA/ASEE Summer Faculty Fellowship Program (W. C. S.), NASA grant NAG 8-409 (J. R. D.), and NASA grant NAG 5-87 and the Center for Astrophysical Sciences of the Johns Hopkins University (W. P. B.). Part of this research was done while J. R. D. was a visiting staff member at the Los Alamos National Laboratory.

REFERENCES

Blandford, R. D., and Cowie, L. L. 1982, *Ap. J.*, **260**, 625.
Cox, D. P. 1972, *Ap. J.*, **178**, 143.
DeNoyer, L. K. 1974, *A.J.*, **79**, 1253.
Dickel, J. R., and Milne, D. K. 1976, *Australian J. Phys.*, **29**, 435.
Dickel, J. R., and Willis, A. G. 1980, *Astr. Ap.*, **85**, 55.
Duin, R. M., and van der Laan, H. 1975, *Astr. Ap.*, **40**, 111.
Fesen, R. A., Blair, W. P., and Kirshner, R. P. 1982, *Ap. J.*, **262**, 171 (FBK).
Green, D. A. 1984, *M.N.R.A.S.*, **211**, 433.
Hester, J. J., Parker, R. A., and Dufour, R. J. 1983, *Ap. J.*, **273**, 219.
Keen, N. J., Wilson, W. E., Haslam, C. G. T., Graham, D. A., and Thomasson, P. 1973, *Astr. Ap.*, **28**, 197.
Landecker, T. L., Roger, R. S., and Dewdney, P. E. 1982, *A.J.*, **87**, 1379.
Lang, K. R. 1978, *Astrophysical Formulae* (New York: Springer-Verlag).
Miller, J. S. 1974, *Ap. J.*, **189**, 239.
Minkowski, R. 1958, *Rev. Mod. Phys.*, **30**, 1048.
Moffet, P. H. 1971, *M.N.R.A.S.*, **153**, 401.
Parker, R. A. R. 1964, *Ap. J.*, **139**, 493.
Smith, M. D., and Dickel, J. R., 1983, *Ap. J.*, **265**, 272.
Straka, W. C. 1986, *Ap. J.*, submitted.
van der Laan, H. 1962, *M.N.R.A.S.*, **124**, 179.

WILLIAM P. BLAIR: Department of Physics, Rowland Hall, The Johns Hopkins University, Baltimore, MD 21218

JOHN R. DICKEL: MS F665, Los Alamos National Laboratory, Los Alamos, NM 87545

ROBERT A. FESEN: Laboratory for Atmospheric and Space Physics, University of Colorado, Campus Box 392, Boulder, CO 80309

WILLIAM C. STRAKA: Lockheed Palo Alto Research Laboratory, Organization 92-20, 3251 Hanover Street, Palo Alto, CA 94303